Int. Conference on Boundary and Interior Layers
BAIL 2006
G.Lube, G.Rapin (Eds)

Numerical simulation of turbulent boundary for stagnation-flow in spray-painting processes

Qiaoyan Ye, Xiaofeng Gui

Institut für Industrielle Fertigung und Fabrikbetrieb
Universität Stuttgart
Nobelstr. 12, 70569, Stuttgart, Germany
e-mail: qyy@ipa.fhg.de

Abstract

The present paper is primarily concerned with modeling complex turbulent wall-bounded flow in spray-painting processes by using a commercial CFD code. Computational results of turbulent channel flow with low Reynolds numbers are compared with DNS data in order to obtain the performance of turbulence models and near wall treatments. The realizable k-ε model with the non-equilibrium wall function and the enhanced wall treatment is employed in the simulation of air flow in spray painting processes. Simulated results are presented with the main focus on the near wall turbulence. Effects of wall-mesh solution and different wall treatments on distributions of velocity and turbulent kinetic energy are analyzed and discussed.

1. Introduction

In order to optimize the painting process, which amounts to a high percentage of fixed and flexible costs in automotive production, numerical simulations of spray painting, especially using high-speed rotary bell and electrostatically supported methods, have been performed [1-6]. Previous numerical studies were mainly concerned with the calculation of the two-phase turbulent flow of the spray jet, the modeling of the electrostatic field including space charge and the prediction of the film thickness distribution on the coated work piece. Reynolds-averaged Navier-Stokes equations (RANS) with k-ε models were used in the computation of the air flow field. However, less attention was paid to the near-wall turbulent flow in the painting process, which is actually quite important for the particle deposition.

It is well known that the RANS approach that is widely used by most CFD codes for industrial applications depends heavily on the turbulence model whose usability is limited for complicated flow fields. Basically, k-ε models and wall functions for wall-bounded flows used by most industrial computation are more suitable for the turbulence flow with high Reynolds numbers because of the isotropic hypothesis in the k-ε models and the special treatment in wall functions.

The considered airflow field in the spray-painting process with high-speed rotary bells is characterized by a complicated turbulent flow, i.e., free jet with spiral and 3-dimensional wake, as well as wall-bounded turbulence boundary with stagnation. The Reynolds number in the free jet region with respect to the bell diameter is about 10^5. However, a re-lamination occurs on the painted work piece, where the Reynolds number based on the thickness of the turbulent boundary is less than 8000. For the final painting characteristics, both the free jet flow and the turbulent boundary on the work

piece play an important role. A detailed investigation on the spray jet flow has been carried out [1,3-5]. The current numerical investigation is aimed at the turbulence boundary of the stagnation airflow. A CFD code (Fluent) based on RANS has to be used because of the complicated turbulent flow in spray-painting processes. A three-dimensional turbulent channel flow is first calculated using different turbulent models with near-wall treatments. The simulated results are compared with the direct numerical simulation (DNS) data [7] in order to obtain the performance of the turbulence models for the current investigation of near-wall flow with low Reynolds numbers. More attention is paid to the velocity distributions and the fluctuation components close to the wall which strongly influence the particle deposition. The complicated three-dimensional turbulent flow is then calculated using a real geometry of the atomizer, a high-speed rotary bell, and simple target geometry, e.g., a flat plate. The influences of the near-wall mesh resolution and the near-wall treatments on the velocity distributions and the turbulent magnitudes close to the target are analyzed. The computational results provide useful information for further studies of particle deposition in spray-painting processes.

2. Comparison of turbulence models with DNS data for channel flow

In the spray-painting process, as mentioned above, the wall-bounded flow on the work pieces is characterized by low Reynolds numbers. Therefore, the performance of the turbulence models with wall treatments is of great important for the current investigation. In order to compare with the DNS data, simulations of turbulent channel flow with 640 000 cells were performed. The length ratio L/H between stream wise and normal direction is 10. The centerline Reynolds number (based on channel half width H/2) is Re_C = 7890. The turbulent mean wall Reynolds number (based on shear velocity u_τ and channel half width) is Re_τ =395. The fully developed turbulent flow was calculated using a one-seventh-power law as the boundary condition of the velocity inlet with relative small turbulent intensity, e.g., 3%. In span wise direction a symmetry condition was used.

Table 1: Used turbulence models

short cut	turbulence model	wall function	near wall model
ske-sw	standard k-ε model	standard wall function	
rke-ne	realizable k-ε model	non-equilibrium wall function	
rke-et	realizable k-ε model		enhanced wall treatment
rsm-et	Reynolds stress model		enhanced wall treatment

Only a few turbulence models from the Fluent code, as shown in Table 1, were chosen for the present numerical study. They are the standard k-ε model proposed by Launder and Spalding [8], realizable k-ε model suggested by Shih et al. [9] and the Reynolds stress model. Since all of these models are primarily valid for turbulent core flows, wall treatment needs to be given to make these models suitable for wall-bounded flows. Here, a standard wall function [8], a two-layer-based, non-equilibrium wall function [10] as well as an enhanced wall treatment [11] were employed. A detailed description of these turbulence models and the wall functions can be found in [12] and in the above mentioned references. Basically, in the wall function approach the viscosity-affected near wall region is not resolved, instead is bridged by some semi-empirical formulas. In the enhanced wall treatment, however, turbulence models are modified to enable the viscosity-affected region to be resolved with a mesh all the way down to the wall, namely the momentum and continuity as well as the k equations are solved up to the wall. A two-layer model is also applied in the enhanced wall treatment for specifying both dissipation rate ε and the turbulent viscosity in the near-wall region. Corresponding to

these two different approaches of the wall treatment, a coarse mesh, for instance, a non-dimensional wall distance $y^+ \approx 30$ ($y^+ = y\, u_\tau/\nu$) at wall-adjacent cells, should be chosen for the application of wall functions, a fine mesh such that $y^+ \approx 1$ at wall-adjacent cells for the application of enhanced wall treatment. Due to the complication of industrial flows, it is difficult for practical applications to keep the optimum wall resolution for a given wall treatment. Therefore, simulations with the selected turbulence models as well as with wall functions were performed in the present study using both coarse and fine meshes, in order to compare the performance of the models.

Figure 1 shows the mean streamwise velocity profiles using different turbulence models together with the fine mesh model. Among these profiles the realizable k-ε model with non-equilibrium wall function deviates significantly from other curves, especially in the middle region of the boundary. In order to compare with the DNS data, non-dimensional mean streamwise velocity profiles scaled by the wall velocity ($U^+ = U/ u_\tau$) are plotted in Fig. 2. It is observed that the data based on the turbulence models in Table 1 with the standard wall function and the enhanced wall treatment agrees very well with the DNS data, where the calculated wall shear stresses τ_ω used for getting wall velocity ($u_\tau = (\tau_\omega/\rho)^{(1/2)}$) are quite close together, $\tau_\omega = 0.39$–0.41 Pa. The realizable k-ε model with the non-equilibrium wall function, however, heavily underestimates the non-dimensional velocity profile in the log region ($y^+ > 30$), since the calculated wall shear stress is about 0.64 Pa which is considerably overestimated.

Similar non-dimensional velocity profiles, but using a coarse mesh, are shown in Fig. 3. Here only the log region is attained. In spite of the coarse mesh the realizable k-ε model and the Reynolds stress model with the enhanced wall treatment can still predict quite good the velocity profiles. A tremendous improvement, however, is obtained for the turbulence model using the non-equilibrium wall function. It is clear that in the case of wall-bounded turbulent flow with low Reynolds numbers numerical results based on the non-equilibrium wall function, for instance, the near wall velocity profiles as well as the wall shear stress are quite sensitive to the wall mesh resolution.

Figure 4 and 5 show the non-dimensional profiles of turbulent kinetic energy k^+ ($k^+ = k/ u_\tau^2$). For the fine grid the turbulence models with the enhanced wall treatment predict the turbulent kinetic energy quite well. The unusual distribution of k^+ with the standard wall function, i.e., increased and constant values of k^+ in the viscosity-affected region ($y^+ < 50$), is not surprising, since the production of k and its dissipation rate ε at wall cells, which are needed for solving the k equation, are estimated using the assumption of local equilibrium that is not valid for the viscosity-affected region. The non-equilibrium wall function, in which a two-layer concept, i.e., a viscous sublayer and a fully turbulent layer, is employed for solving the k equation at the wall cells, improves the distribution of k^+ in the viscosity-affected region ($y^+ < 50$). However, compared with DNS data a significant deviation can still be observed. It should be noticed that the dimensional k obtained using the non-equilibrium wall function is actually larger than that using the enhanced wall treatment. The lower pick value of k^+ for the curve rke-ne is due to the overestimated wall velocity in the non-equilibrium wall function.

For a coarse grid, as shown in Fig. 5, data of k^+ using both the wall functions and the enhanced wall treatment are poorly estimated, especially for the enhanced wall treatment in the region of $30 < y^+ < 100$. Obviously, the effect of the grid resolution on the k distribution is larger than that on the mean velocity distribution (see Fig. 3).

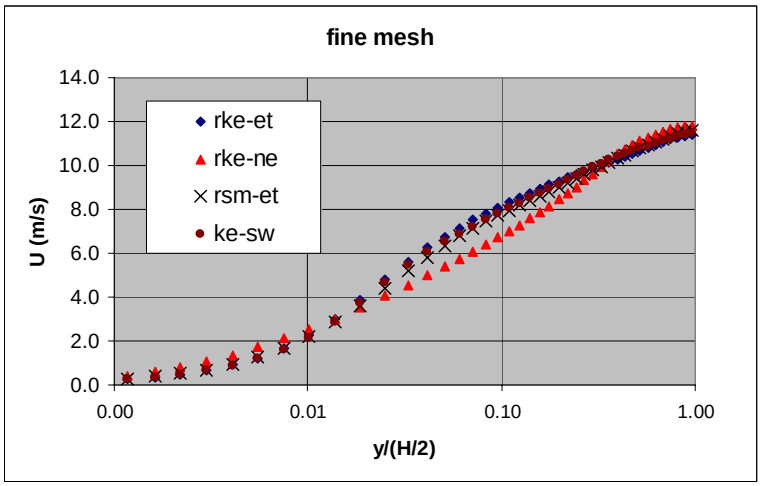

Fig. 1: Mean streamwise velocity profiles using fine mesh and different turbulence models.

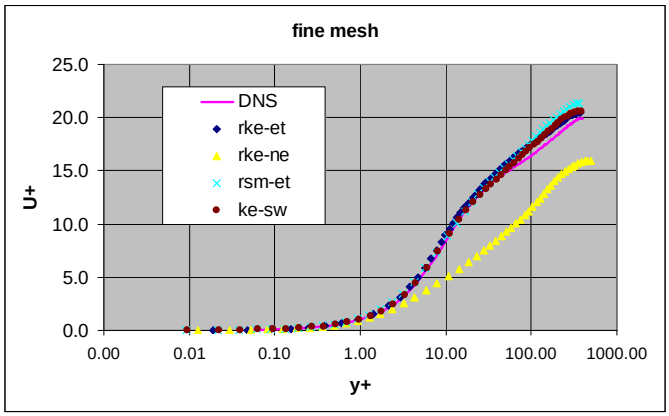

Fig. 2: Comparison of non-dimensional mean streamwise velocity profiles using fine mesh.

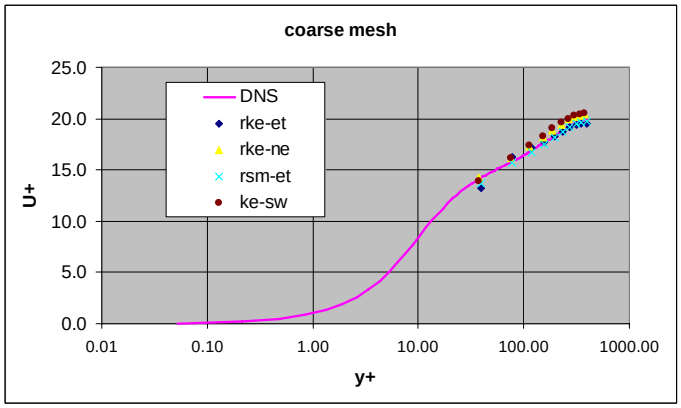

Fig. 3: Comparison of non-dimensional mean streamwise velocity profiles using coarse mesh.

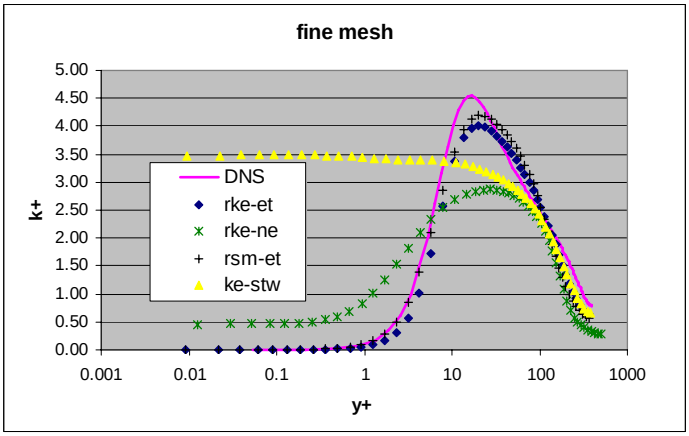

Fig. 4: Comparison of non-dimensional k^+ profiles using fine mesh.

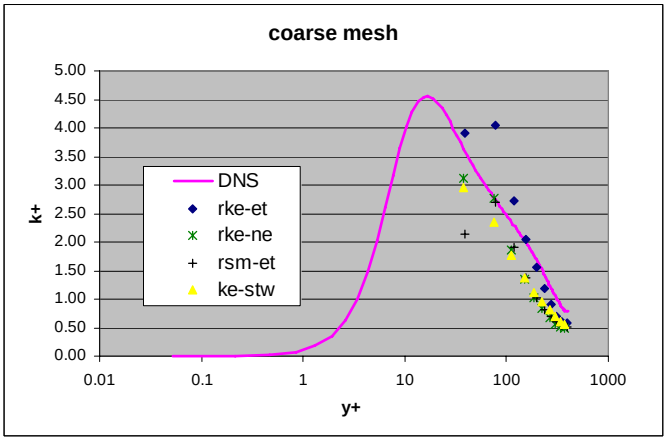

Fig. 5: Comparison of non-dimensional k^+ profiles using coarse mesh.

3. Simulation of a turbulent boundary in spray painting processes

3.1 Computational details

In the section above, the performance of different turbulence models and near wall treatments in the Fluent code is compared by using DNS data of channel flow with low Reynolds number. The practical airflow field in the spray-painting processes is quite complicated, which is characterized by free jet with spiral and 3-dimentional wake with high Reynolds number as well as wall-bounded flow with low Reynolds number on the painted object. The Reynolds stress model is usually recognized as the more suitable model for anisotropic turbulent flows, however, it is difficult to get a convergent solution for the present complex flow. Therefore, the realizable k-ε model that is believed to give appreciable improvement over other k-ε models for a wide range of flows, e.g., free flows including jet and mixing layers, channel and boundary layer flows, etc., was applied. Two different near wall treatments, i.e., the non-equilibrium wall function that is widely used for industrial computation and the enhanced wall treatment, as well as different wall-mesh resolution, as shown in Table 2, were used in order to study more detailed the wall-bounded flow in spray painting processes. The pressure gradient effect in both near wall approaches was taken into account.

The computational domain is 2 x 2 x 1.7 m^3, including the rotary bell atomizer and a target plate with the size of 1 x 1m^2. The distance between the atomizer and the target plate is 230 mm. A hybrid unstructured mesh with half a million cells was used. The local mesh refinement, especially in the region downstream of the bell and on the bodies of the bell and the target plate, was performed. According to our previous study [1,5], the main structure of the spray jet airflow is quasi stable. A quasi-steady three-dimensional turbulent airflow in the spray jet is therefore applied in this study. The numerical scheme used here is of second order accuracy in space.

Table 2: Near wall treatments

short cut	near wall treatment	wall cell resolution [mm]
rke-et-fm	enhanced wall treatment	0.2
rke-et-cm	enhanced wall treatment	1
rke-ne-fm	non-equilibrium wall function	0.2
rke-ne-cm	non-equilibrium wall function	1

3.2 Results and discussion

The numerical results are presented and analyzed in this section with the primary focus on the turbulent wall-bounded flow on the target plat. It is, however, necessary to at first show the whole flow field of the spray jet, in order to understand the process.

Figure 6 shows the velocity vector in a cross section that was created through the center of the jet. The shaping air is delivered through the air nozzles behind the bell with very high speed (220 m/s) and directed along the outer surface of the bell. At the bell edge, the tangential velocity is 130 m/s due to the rotary speed and its axial velocity is about 35 m/s. In order to provide an insight into the whole jet flow field, only the velocity in the range of 0 - 10 m/s is displayed. Large vortices can be seen located downstream the bell edge. Along the spray axis a negative pressure region is formed because of the spiral flow (see Fig. 7), and the high level of turbulence downstream the bell is caused by the vortex shedding, both which result in a flow recirculation in the centre of the spray jet. The thickness of

turbulent boundary near the target plate is about 25 mm.

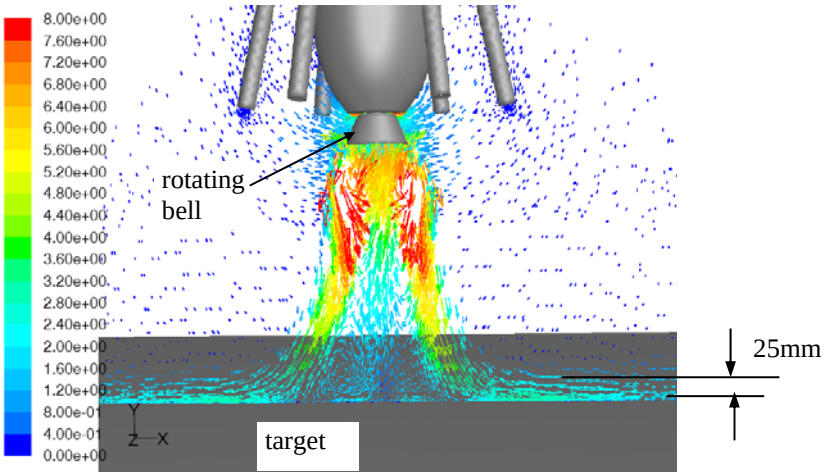

Fig. 6: Velocity vector coloured by velocity magnitude in m/s in a cross section.

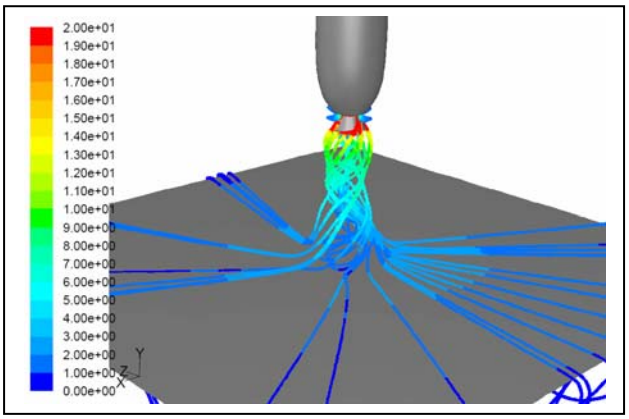

Fig. 7: Streamlines coloured by velocity magnitude in m/s in the main region of the jet flow.

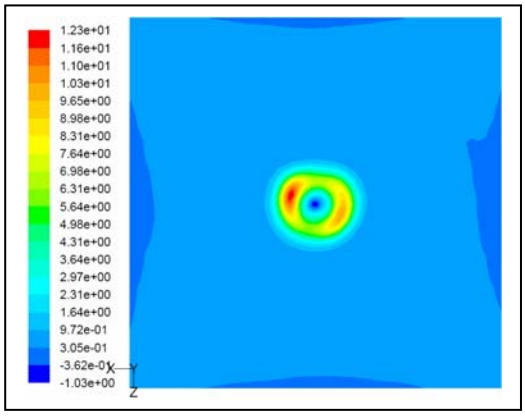

Fig. 8: Contours of pressure coefficient on the target.

In the following computational results near the target wall are presented. A typical pressure distribution on the target is depicted in Fig. 8. The negative pressure is located at the center of the target. Away from the center the maximum pressure is reached close to the stagnation point. An adverse pressure gradient is formed in this region.

The velocity distributions on the target plate with fine and coarse meshes using different wall treatments are shown in Fig. 9 and 10. The corresponding y^+ in the wall cells are $0 < y^+ < 4$ for the fine mesh and $0 < y^+ < 13$ for the coarse mesh. It can be seen that the characteristic shape of the velocity contours are quite close, especially in Fig. 9a, 9b and 10a.

However, for the fine mesh the non-equilibrium wall function predicts the velocity in the wall cells more than two times than that in the enhanced wall treatment, which is identical to the analysis of the velocity profiles quite close to the wall (Fig. 1) in the simulation of the channel flow. Although the maximum velocities in Fig.10a and 10b are similar, a significant spread of the velocity in the wall cells using the non-equilibrium wall function is observed.

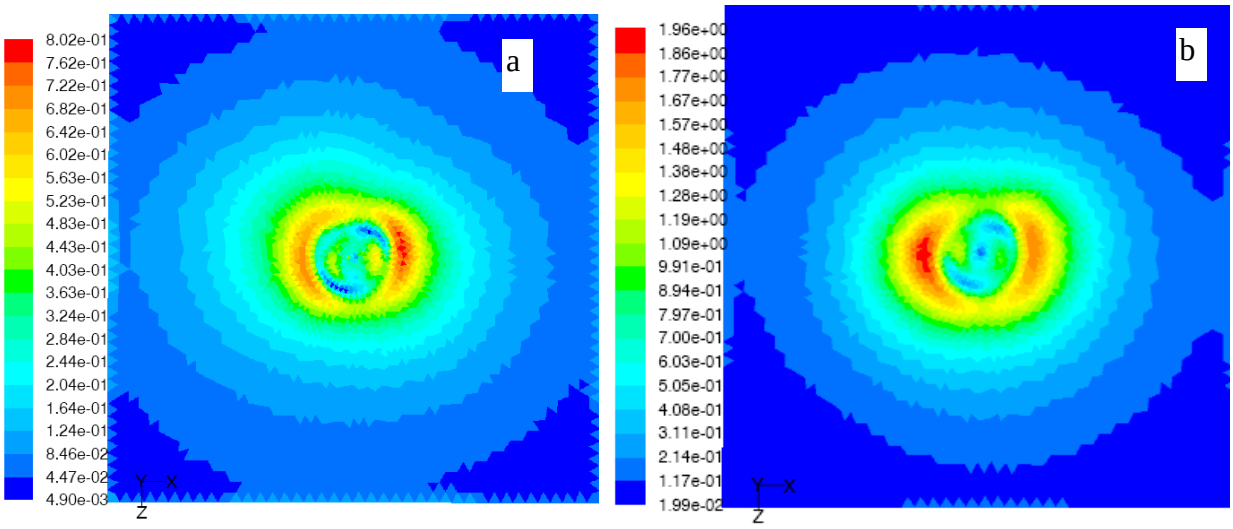

Fig. 9: Velocity contours in m/s in the wall-adjacent cells with a fine mesh using different wall treatments. a): enhanced wall treatment, b): non-equilibrium wall function.

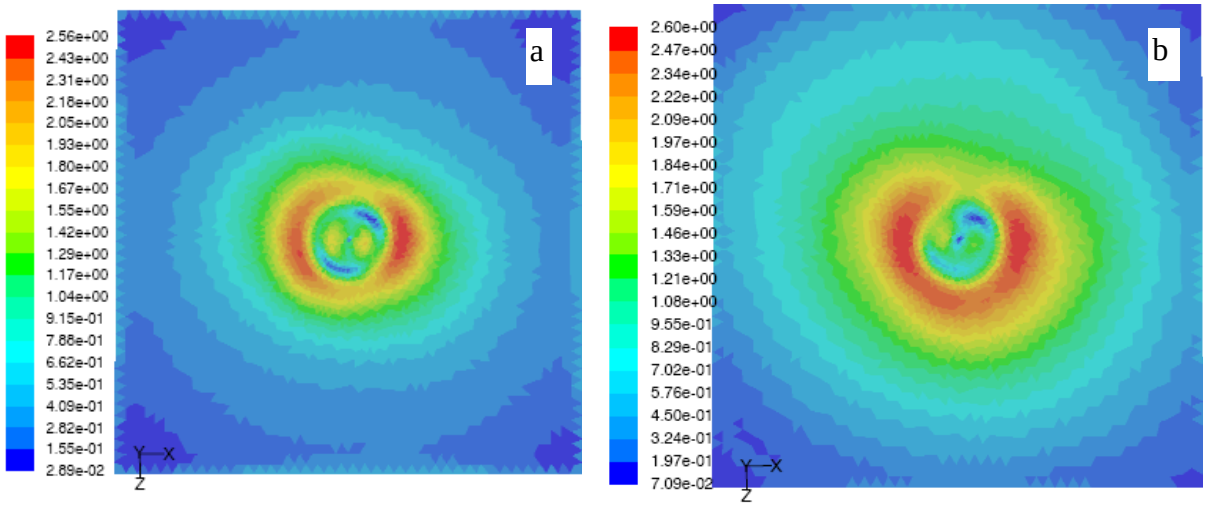

Fig. 10: Velocity contours in m/s in the wall-adjacent cells with a coarse mesh using different wall treatments. a): enhanced wall treatment, b): non-equilibrium wall function.

As noted earlier, our main interests here are not only the velocity distributions but also the profiles of turbulent kinetic energy k in wall-bounded flow. For better comparison, profiles of velocity magnitude and k along the line that was created parallel to the target wall with a wall distance of 1 mm and through the spray center are shown in Fig. 11 and 12. Both fine and coarse mesh models can attain the wall resolution of the line. In opposition to the results shown in Fig. 9 and 10, the velocity using the enhanced wall treatment is higher than that using the non-equilibrium wall function for this wall distance, which can also be proven in the above simulation of channel flow, where in the middle region of the wall boundary the non-equilibrium wall function underestimated the velocity. In contrast to the results from Fig. 11, the k profiles in Fig. 12 obtained using the non-equilibrium wall function are significantly larger than those using the enhanced wall treatment, which seems contrary to the results in Fig. 4. However, keeping in mind that the wall shear stress used for scaling k^+ in Fig. 4 for the non-equilibrium wall function was overestimated compared with DNS data, the results in Fig. 12 are identical to those in Fig. 4.

Alternatively, the velocity and turbulent kinetic energy profiles across the turbulent boundary on the target plate, namely along the line that was created 0.12 m away from the spray axis center and perpendicular to the wall, are shown in Fig. 13 and 14. It is found that the non-equilibrium wall function gives higher velocity and k in the region quite close to the wall but lower velocity and k far away from the wall.

In addition, Figures 11 to 14 indicate that the influence of mesh resolution on the velocity and k profiles is significant for the non-equilibrium wall function. For the enhanced wall treatment, the predicted turbulent kinetic energy is somewhat more sensitive (see Fig. 14) to the wall mesh resolution than the calculated velocity profile. It should be pointed out here that the present coarse mesh in the wall region is still too fine for the application of the non-equilibrium wall function. In order to obtain the optimum wall resolution ($y^+ > 30$), the space of the first wall cell will be about 3 mm that is, however, obviously too coarse for an accurate prediction of particle deposition in spray-painting processes.

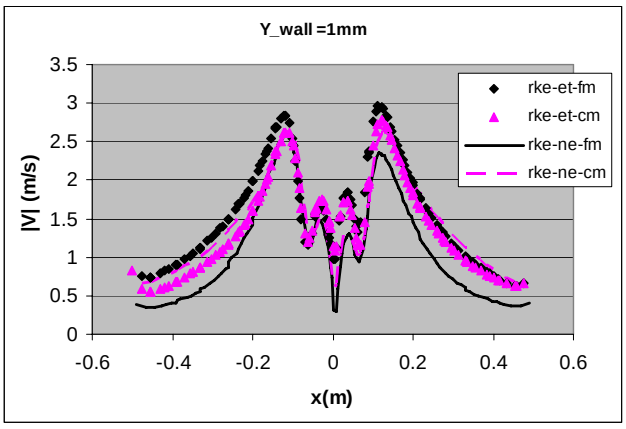

Fig. 11: Velocity profiles using different wall treatments and different mesh resolutions.

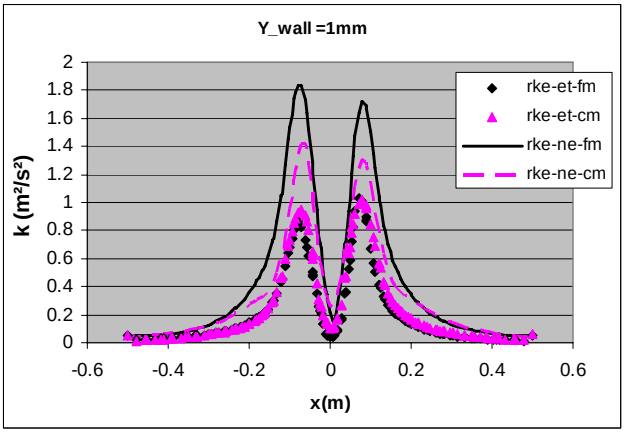

Fig. 12: Profiles of turbulent kinetic energy using different wall treatments and different mesh resolutions.

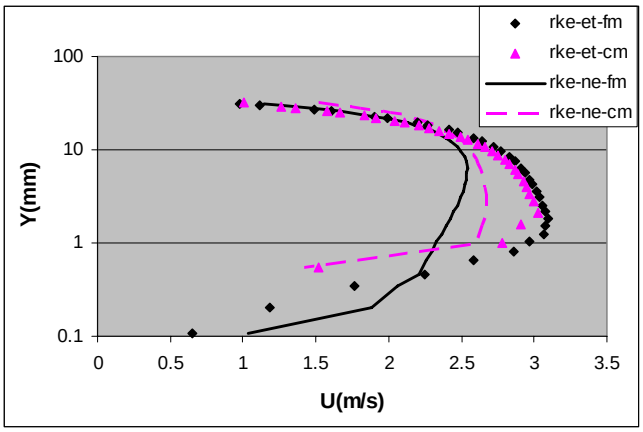

Fig. 13: Velocity profiles across the wall boundary using different wall treatments and different mesh resolutions.

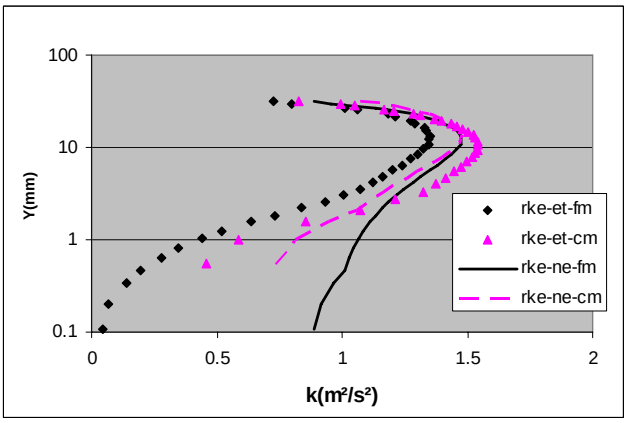

Fig. 14: Profiles of k across the wall boundary using different wall treatments and different mesh resolutions.

4. Concluding remarks

Although, as mentioned in the introduction above, many numerical simulations of spray painting processes have been carried out in recent years, less attention has been paid to the flow field close to the painted solid surface, where the velocity is strongly reduced compared with spray jet and wake flow. In this paper numerical simulations with a realizable k-ε model and two wall treatments as well as different wall mesh resolutions have been performed to predict the air flow in real spray painting process with a high-speed rotary bell. It is found that the enhanced wall treatment is insensitive to the grid spacing near the wall, which is identical to the present results of channel flow and to the results obtained by Chen and Patel [11] for other complex flows. The predicted velocity and the turbulent kinetic energy close to the wall using the non-equilibrium wall function deviate considerably from the results using the enhanced wall treatment and are quite sensitive to the near wall mesh resolution. Based on the comparison of the computational results of turbulent channel flow with DNS data, we believe that the enhanced wall treatment predicts more reasonably the flow field for the spray painting processes than the non-equilibrium wall function that was employed by some researchers [1,13].

Of course, the validation of the computational results for this particular complex near wall flow involving stagnation, pressure gradient and swirl by using DNS data of channel flow is somewhat weak. More comprehensive investigations should be carried out. Unfortunately, for such near wall flow it is quite difficult to get accurate flow field data by means of experiments, for instance, measurement using Laser-Doppler anemometry. For the Reynolds stress model that is recognized as the more suitable model for anisotropic turbulent flow, the stability of iteration and the convergent performance should be improved for the application of complex turbulent flows. In future, it is necessary to implement other turbulence models with improved wall treatments, for instance, v^2-f models based on Durbin´s elliptic relaxation concept [14] that are considered to give a better performance for the flow with impingement. Further studies on particle deposition in spray painting processes using the current computational results of the near wall flow are required, which is an

alternative approach for testing the selected turbulence models and the corresponding wall treatments.

References

[1] Q. Ye, J. Domnick, A. Scheibe, K. Pulli: Numerical Simulation of the Electrostatic Spray-painting Process in the Automotive Industry. High-Performance Computing in Science and Engineering'04, Springer-Verlag Berlin, Heidelberg, 2004, pp. 261-275.

[2] Q. Ye, J. Domnick: On the simulation of space charge in electrostatic powder coating with a corona spray gun. Powder Technology 135-136 (2003) 250-260.

[3] J. Domnick, A. Scheibe, Q. Ye: The simulation of the electrostatic spray painting process with high-speed rotary bell atomizers. Part I: Direct charging, Part. Part. Syst. Charact. 22 (2005) 141-150.

[4] J. Domnick, A. Scheibe, Q. Ye: The simulation of the electrostatic spray painting process with high-speed rotary bell atomizers. Part II: External charging, accepted by Part. Part. Syst. Charact. in 2006.

[5] Q. Ye, A. Scheibe, T. Steinhilber, J. Domnick: Unsteady numerical simulation of the air flow field in the spray painting process using high-speed rotary bell atomizers, submitted to HLRS-Workshop, Stuttgart, 05-06 Oct. 2006.

[6] S.A. Colbert, R.A. Cairncross: A discrete droplet transport model for predicting spray coating patterns of an electrostatic rotary atomizer. J. of Electrostatics 64 (2006) 234-246.

[7] J. Kim, P. Moin, R. Moser: Turbulence statistics in fully developed channel flow at low Reynolds number. J. Fluid Mech. 177 (1987) 133-166.

[8] B. E. Launder and D. B. Spalding: The numerical computation of turbulent flows. Computer Methods in Applied Mechanics and Engineering, 3 (1974) 269-289.

[9] T.-H. Shih, P. W. W. Liou, A. Shabbir, Z. Yang and J. Zhu: A new k-ε Eddy-viscosity model for high Reynolds number turbulent flow- Model development and validation. Computers Fluids, 24(3): 227-238 (1995).

[10] S.-E. Kim, D. Choudhury, and B. Patel: Computations of complex turbulent flows using the commercial code FLUENT. In ASME FED Vol. 217, Separated and Complex Flows. ASME, 1995.

[11] H. C. Chen and V. C. Patel: Near-wall turbulence models for complex flows including separation. AIAA Journal, 26(6): 641-648 (1988).

[12] Fluent User's Guide

[13] J. E. McCarthy, Jr, and D. W. Senser: Numerical model of paint transfer and deposition in electric air sprays. Atomization and Sprays, vol.16. pp.195-222 (2006).

[14] M. Behnia, S. Parniex, P. A. Durbin: Prediction of heat transfer in an axisymmetric turbulent jet impinging on a flat plate. Int. J. Heat Mass Transfer 41, 1845-1855 (1998).